Çukurova Üniversitesi
Mühendislik Fakültesi Dergisi
Çukurova University
Journal of the Faculty of Engineering
ISSN: 2757-9255 CİLT/VOLUME: 41 SAYI/ISSUE: 3 EYLÜL/SEPTEMBER 2026

CFD Investigation of the Effect of Jet-Surface Distance on Thermal Performance in Inclined Jet Impingement Cooling

Haydar KEPEKÇİ [1,a]

[1]*Istanbul Gelisim University, Faculty of Engineering-Architecture, Department of Mechatronics Engineering, Istanbul, Türkiye*

[a]***ORCID**: 0000-0002-0037-8332*

Article Info
Received : 27.02.2026
Accepted : 16.09.2026
DOI: 10.21605/cukurovaumfd.1898969

Corresponding Author
Haydar KEPEKÇİ
hikepekci@gelisim.edu.tr

Keywords
Jet impingement cooling
Inclination angle
Jet-to-wall spacing
Computational fluid dynamics
SST k–ω model

***How to cite:** KEPEKÇİ, H., (2026). CFD Investigation of the Effect of Jet-Surface Distance on Thermal Performance in Inclined Jet Impingement Cooling. Cukurova University, Journal of the Faculty of Engineering, 41(3), 679-692.*

ABSTRACT

This study numerically investigates the influence of geometric parameters on heat transfer in inclined jet impingement cooling. Twenty configurations were analyzed for H/D ratios of 3–6 and jet inclination angles of 0°–60° at Re = 15,000. Two-dimensional steady turbulent simulations were performed using the SST k–ω model within a CFD framework. Results show that both the H/D ratio and inclination angle significantly affect thermal performance. The average Nusselt number increased from 4.09–4.49 at H/D = 3 to 5.05–6.83 at H/D = 6. The heat transfer coefficient rose from 19.82 W/m²K at H/D = 3 and 0° to 33.08 W/m²K at H/D = 6 and 60°. Enhanced turbulence and flow mixing improved heat transfer. The most favorable thermal performance among the investigated cases was observed at H/D = 5–6 and inclination angles of 45°–60°, providing useful guidance for the geometric optimization of inclined jet impingement cooling systems.

Eğimli Jet Çarpma Soğutmasında Jet-Yüzey Mesafesinin Isıl Performans Üzerindeki Etkisinin CFD ile İncelenmesi

Makale Bilgileri
Geliş : 27.02.2026
Kabul : 16.09.2026
DOI: 10.21605/cukurovaumfd.1898969

Sorumlu Yazar
Haydar KEPEKÇİ
hikepekci@gelisim.edu.tr

Anahtar Kelimeler
Jet çarpma soğutma
Eğim açısı
Jet-duvar mesafesi
Hesaplamalı akışkanlar dinamiği
SST k–ω modeli

***Atıf şekli:** KEPEKÇİ, H., (2026). Eğimli Jet Çarpma Soğutmasında Jet-Yüzey Mesafesinin Isıl Performans Üzerindeki Etkisinin CFD ile İncelenmesi. Çukurova Üniversitesi, Mühendislik Fakültesi Dergisi, 41(3), 679-692.*

ÖZ

Bu çalışmada, eğimli jet çarpma soğutma akışlarında geometrik parametrelerin ısı transferine etkileri sayısal olarak incelenmiştir. H/D oranları 3–6 ve jet eğim açıları 0°–60° olan toplam 20 konfigürasyon, Re = 15.000 sabit tutularak analiz edilmiştir. Çözümler, iki boyutlu kararlı türbülanslı akış koşullarında SST k–ω modeli kullanılarak CFD ortamında gerçekleştirilmiştir. Sonuçlar, H/D oranı ve eğim açısının ısı transferini belirgin biçimde etkilediğini göstermiştir. Ortalama Nusselt sayısı H/D = 3 için 4,09–4,49 aralığından H/D = 6 için 5,05–6,83 aralığına yükselmiştir. Isı transfer katsayısı ise H/D = 3 ve 0° için 19,82 W/m²K'den, H/D = 6 ve 60° için 33,08 W/m²K'ye çıkmıştır. Artan türbülans yoğunluğu ve akış karışımı ısı transferini iyileştirmiştir. İncelenen durumlar arasında en uygun termal performans, H/D = 5–6 ve 45°–60° eğim açılarında gözlemlenmiştir. Bu da eğimli jet püskürtmeli soğutma sistemlerinin geometrik optimizasyonu için faydalı bir kılavuz sunmaktadır.

1. INTRODUCTION

The reliable and efficient operation of systems with high heat flux requires an effective thermal management strategy. The increasing power densities of electronic components and rising performance expectations in engine and turbine systems have led to the limitations of traditional cooling methods [1]. In this context, jet impingement cooling is an advanced cooling technique that reduces the boundary layer thickness by directly impinging a high-speed flow onto the surface, resulting in significantly higher heat transfer coefficients than classical convective methods [2]. The basic principle of jet impingement cooling is to reduce the boundary layer thickness and increase the temperature difference between the surface and the fluid by directly impinging the high-speed flow on the target surface. This effect enables much higher local heat transfer coefficients (h) than in classical convective cooling or channel cooling systems [1]. Therefore, jet impingement cooling is widely preferred in various applications, including the cooling of gas turbine blades, thermal management of electronic circuits, cooling of automotive components, and temperature balancing in fuel cells [3].

However, heat transport performance in jet impingement systems depends not only on the jet speed or Reynolds number but also on the jet-to-wall distance (H/D ratio), jet inclination angle (θ), nozzle geometry, and surface conditions [4]. If the jet is too close to the surface, the flow impinges on the wall before it has had a chance to develop, leading to premature flow separation. Conversely, if the jet-to-wall distance is too large, the jet core weakens, and the flow energy dissipates, limiting heat transport. Similarly, when the jet impinges on the wall at an angle, the flow slides along the wall, creating secondary vortices and enhancing the turbulent surface mixing. Therefore, the combination of jet inclination angle and jet-to-wall distance plays a critical role in maximizing heat transfer within the investigated parameter range.

There are studies on this subject in literature. Xu et al. investigated the flow field and heat transfer characteristics of jets existing specially shaped orifices [5]. In this context, they classified and compared variable-diameter, irregular-geometry, and swirl nozzle types. They evaluated both experimental and CFD-based literature to examine the effects of different geometries on flow structure, turbulence intensity, and temperature distribution. According to the results obtained in the literature, the main reason for this performance increase is that specially shaped nozzles intensify the turbulence level by directly affecting the jet momentum, causing premature breakdown of the boundary layer at the target surface, and increasing the local heat transfer coefficient by creating high velocity gradients in the collision region. Consequently, they emphasized that specially shaped orifices provide significant improvements in both average heat transfer and temperature uniformity compared with conventional circular nozzles in jet-cooling applications. Alnak and Karabulut numerically demonstrated that surface geometry and jet inlet parameters are decisive in heat transfer in jet impingement applications, and that geometries such as inverted semicircles can significantly increase the average Nusselt number compared to flat surfaces [6]. Yang et al. investigated the flow structure and heat transfer characteristics of a jet impingement system with enlarged jet holes experimentally and numerically [7]. In their study, they aimed to evaluate the flow deflection behavior and its effects on heat transfer by varying the extended lengths of the jet holes (1.0d–2.5d) under flow conditions with Re = (1.0–3.0) × 10^4. As a result of their experimental and CFD-based analyses, they found that the enlarged jet holes increased the local heat transfer by approximately 36% and significantly homogenized the heat transfer distribution. They also stated that the enlarged jet configuration provided heat transfer that was more than 10% higher than that of the classical design at the same pumping power, and that this approach has high potential for future engineering applications.

Cademartori and colleagues investigated new cooling configurations for an industrial galvanizing line using the slot-jet impingement cooling technique [8]. In their research, they developed a CFD-based numerical model, validated it with experimental data, and investigated the effects of different jet numbers and jet-to-wall distances on heat transfer. The aim of their study was to understand the effects of slot-jet geometry on cooling uniformity and surface quality, and to propose an alternative design to the existing circular-jet system. Consequently, they concluded that increasing the jet-to-wall distance provides a more uniform temperature distribution, reduces mechanical stress, and results in higher product quality, making slot-jet impingement a more effective cooling strategy in galvanizing lines. Lin et al. systematically investigated the heat transfer behavior of a confined slot-jet impingement experimentally [9]. In their study, the researchers aimed to investigate the effects of different jet Reynolds numbers (Re = 190–1537) and jet-separation distance ratios (H/W = 1–8) on the stagnation and mean Nusselt numbers on the heated target surface. As a result of their investigation, they found that the heat transfer performance increased

significantly with increasing jet Reynolds number, but the effect of the separation distance was limited. In addition, they proposed two new empirical correlations for stagnation and the mean Nusselt number and found that these correlations agreed with the experimental data within 4.56% and 7.88%, respectively. Kaewchoothong et al. numerically investigated the effects of jet-target gap on flow and heat transfer in rotating impinging micro-slot jets [10]. In their study, the researchers aimed to evaluate the effect of jet-target distance on heat transfer performance using the k-ε turbulence model over the range Re = 5000–20000 and L/D ratios of 1–6. Their analysis showed that the average Nusselt number was 32.9–54.2% higher for the L/D = 1 configuration compared to other configurations, and this effect was due to the vortex density at high speed and direct flow impingement. They also stated that as the L/D ratio increases, jet flow acceleration and the TKE distribution at the wall decreases, resulting in lower Nu values and a wider stagnation zone. It has been experimentally shown by Keleş and Özmen that the heat transfer performance in jet impingement flows varies with parameters such as Reynolds number and jet-plate distance, and that increasing the Reynolds number increases the Nusselt number, while increasing the jet-plate distance reduces it [11].

Benmouhoub and Mataoui numerically investigated the turbulent flow and heat transfer behavior of a slotted jet impinging on a moving wall [12]. In their study, they aimed to evaluate the effects of different jet-to-wall velocity ratios (Rsj) and Reynolds numbers on the flow field and the Nusselt number using a CFD model based on the finite-volume method. Their analysis revealed that significant asymmetries emerge in the stagnation region with increasing Reynolds number and wall velocity, and that the average Nusselt number attains a maximum value around Rsj = 1.5. They also noted that at high velocity ratios, the flow becomes fully separated from the wall, leading to reduced heat transfer and a delay in the onset of the pressure-induced Coandă effect. Singh et al. numerically investigated the heat transfer behavior of jet impingement in a system comprising nine square jets [13]. In their study, they aimed to evaluate the effects of changes in Reynolds number (Re), inter-jet distance (S/D), and separation distance (H/D) on heat transfer by comparing different turbulence models (Standard, RNG, Realizable k-ε, and SST k-ω) with the RANS approach in the CFD-based Fluent software. As a result of their analysis, they found that the SST k-ω model showed the highest agreement with the experimental data, and the average heat transfer coefficient decreased from 210 to 193 W/m²K when the H/D ratio increased from 6 to 10. They also concluded that the heat transfer reached optimal values at S/D = 3, and that as the S/D ratio decreased, the jets merged into a single powerful jet. Shin et al. investigated the effects of channel height on flow and heat transfer in channel impingement cooling systems experimentally and numerically [14]. In their study, the researchers performed simulations using the SST k-ω turbulence model with water, covering Re = 2000–8600 and channel heights of 3-6 mm, with an array of 11 jets, each with a diameter of 0.8 mm. As a result of their investigation, they found that the average Nusselt number increases with the Reynolds number and decreases with the channel height. The developed correlation agrees with the experimental data within a 4.31% margin of error. They also stated that heat transfer in the stagnation region decreases with increasing channel height, whereas at high jet speeds, the wall-jet effect strengthens heat transfer between the stagnation zones. These findings provide important design guidance for optimizing channel impingement cooling configurations. Olsson et al. numerically investigated the heat transfer behavior of a slot jet impinging on a cylindrical tube placed on a solid surface in a semi-enclosed space [15]. In their CFD study, they employed the SST turbulence model to investigate the impact of various Reynolds numbers (23,000–100,000), jet-to-cylinder distances (H/D = 2–8), and surface curvature ratios (d/D = 0.29–1.14) on heat transfer. Their analysis revealed that both the average and stagnation Nusselt numbers increased with increasing Reynolds number and surface curvature, while the effect of the jet-to-cylinder distance was limited. They also found that heat transfer reached maximum values at the top of the cylinder and the exit region, and minimum values in the separation region. Additionally, they found that the correlations obtained could be used in industrial heat treatment designs.

Culun et al. numerically investigated the synergistic heat transfer behavior of multiple jet impingement [16]. In their study, they aimed to evaluate the effects of different jet geometries, arrangements, jet-to-jet spacing ratios (Xn/d), and jet-to-target distances (x/d) on heat transfer using ANSYS-CFX software. As a result of their analysis, they found that when Xn/d = 2, the jets behave like channel flow, in which case the stagnation effects decrease, and the heat transfer increases towards the channel exit. They also concluded that square jets provide a higher Nusselt number than circular jets, and that the jet arrangement shape is the weakest parameter for heat transfer. Kumar et al. numerically investigated the heat transfer and pressure drop behavior of a straight slot jet in a square channel using TiO_2/H_2O nanofluid [17]. In their study, they aimed to evaluate the thermohydraulic performance by varying the jet height (Hjet/Dhd = 0.3–0.6), aperture

ratio (Pspan/Dhd = 0.18–0.45), and flow rate (Pstream/Dhd = 0.88–1.30) parameters in the range Re = 8000–17000 using the RNG k-ε turbulence model. As a result of their analysis, they found that the TiO_2/H_2O nanofluid provided a significant improvement in heat transfer, with an approximately 6% higher Nusselt number and a 3% lower error rate compared to pure water. They also observed that the optimum configuration was achieved at Hjet/Dhd = 0.5, Pspan/Dhd = 0.3, and Pstream/Dhd = 0.97, at which point THPP reached its highest efficiency in the range of 0.97–1.04.

Molana and Banooni comprehensively reviewed heat transfer processes with liquid impingement jets and existing research in this area [18]. In their study, the researchers aimed to evaluate the effects of flow parameters and nanofluid additives on jet-cooling performance by compiling various Nusselt-number correlations. Their investigation revealed that the Nusselt number increases with increasing Reynolds number and nanoparticle volume fraction, while nanofluids significantly increase the pressure drop. They also noted that nanoparticle effects in multi-jet systems have not been adequately investigated, and that new models and experimental data are needed to develop this area. Uddin et al. conducted a comprehensive literature review examining the flow dynamics and heat transfer characteristics of single circular and slotted jets [19]. In their study, the researchers aimed to compare the effects of Reynolds number, nozzle geometry, and jet-target spacing on the distribution of the Nusselt number. Their review revealed that existing correlations have been developed specifically for circular jets and that sufficiently accurate models for slot-jet impingement have been lacking. Furthermore, they found that the formation of primary and secondary peaks in the Nusselt distribution is closely related to turbulent structures. They also emphasized that, given the limited number of high-accuracy LES/DNS studies, machine learning-based approaches could help improve understanding of these complex flow structures in the future.

Despite the considerable number of experimental and numerical studies, previous investigations have generally focused on individual parameters, such as nozzle geometry, Reynolds number, jet-to-wall distance, or a single jet inclination angle. Consequently, a comprehensive understanding of the combined influence of jet inclination angle and jet-to-wall distance on heat transport remains limited. Furthermore, the wide variation in Reynolds numbers among previous studies makes direct comparisons difficult. To address these limitations, the present study employs a CFD-based numerical approach to systematically investigate the combined effects of jet-to-wall distance (H/D = 3, 4, 5, and 6) and jet inclination angle (θ = 0°, 15°, 30°, 45°, and 60°) while maintaining a constant Reynolds number of 15,000. The Nusselt number, heat transfer coefficient (h), and temperature distributions are evaluated for all cases. In this context, the present study contributes to the literature by providing a systematic assessment of the combined influence of jet inclination angle and jet-to-wall distance on the thermal performance of inclined jet impingement systems.

2. MATERIALS AND METHODS

2.1. Design

In this study, the effects of different jet-to-surface distances (H/D ratios) and inclination angles (θ) on heat transfer performance are numerically investigated. The designed model represents a two-dimensional rectangular channel configuration with a single circular jet exit. The jet exit is located at the top of the channel and directed towards the heated plane at the bottom surface. Analyses have been conducted by varying only the H/D ratio and the jet inclination angle while keeping the system geometry unchanged. Thus, the effects of the jet-to-wall distance and inlet jet inclination on the flow structure and heat transfer characteristics can be investigated independently of other geometric and operating parameters. The geometry was created using CAD-based modeling software and exported in STEP format, suitable for CFD analysis using the finite volume method. The jet exit diameter was kept constant (D = 30 mm), while the jet-to-heated wall distance was evaluated at four different levels (H/D = 3, 4, 5, and 6). For each H/D ratio, five different jet inclination angles (θ = 0°, 15°, 30°, 45°, and 60°) were imposed by changing only the inlet velocity direction while keeping the nozzle geometry unchanged. Therefore, the computational geometry remained identical across all inclination angles, and only the orientation of the inlet velocity vector was modified, yielding a total of 20 numerical cases. The heated surface length was kept constant at 120 mm, and the jet exit was positioned symmetrically with respect to the flow axis. In all models, the wall thickness and jet diameter remained constant, whereas only the inlet velocity vector orientation and the jet-to-wall distance were varied. This approach allows an isolated investigation of the effects of these parameters on

the flow regime, turbulence structure, and heat transfer coefficient. Figure 1 illustrates the computational domain together with the definition of the jet inclination angle (θ).

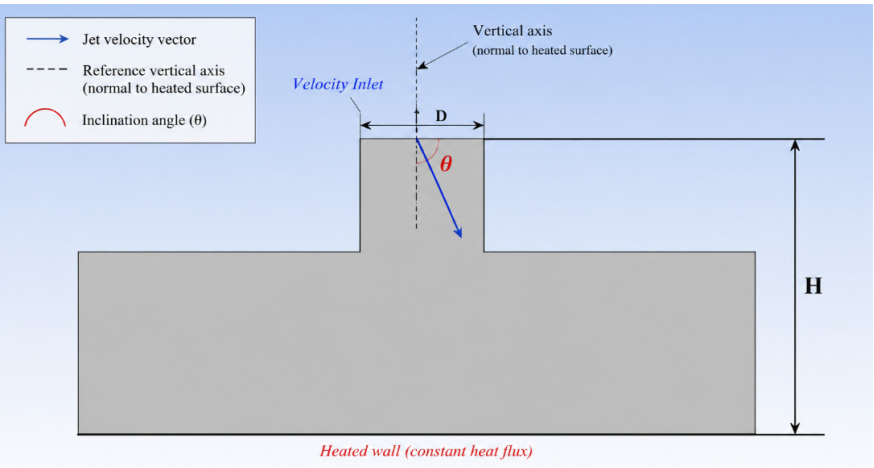


Figure 1. Schematic of the computational domain and definition of geometric parameters

2.2. Meshing

To improve the accuracy and stability of the numerical analyses, a detailed computational mesh was generated for all jet impingement geometries using the ANSYS Meshing module. The computational domain included the jet inlet, the target surface, and the surrounding walls. A structured quadrilateral mesh was employed to accurately capture the strong velocity and temperature gradients developed within the impingement region. Since quadrilateral elements can be preferentially aligned with the main flow direction, they provide improved numerical accuracy and better resolution of the boundary layer compared with unstructured meshes. In addition, local mesh refinement was applied in the jet inlet region and near the heated wall to accurately resolve the impinging jet and wall-jet flow. Inflation layers were generated along the heated wall to maintain wall y^+ values below 1, ensuring that the viscous sublayer was fully resolved. This near-wall resolution is recommended for the SST k–ω turbulence model because it enables accurate prediction of wall shear stress, boundary-layer development, and convective heat transfer without relying on wall functions. The representative computational mesh adopted in the present study is illustrated in Figure 2.

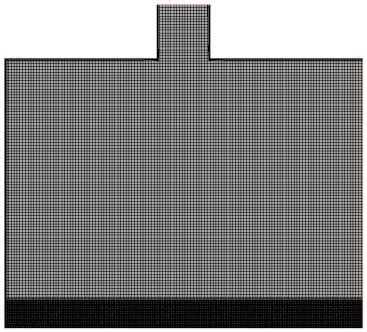


Figure 2. Computational mesh of the jet impingement domain

A mesh independence study was performed for the most critical operating condition (H/D = 6 and θ = 60°), where the highest heat transfer performance was obtained. Three different mesh densities were generated and compared using the average Nusselt number as the evaluation criterion. As presented in Table 1, the predicted average Nusselt number changed by less than 1% between the medium and fine meshes, indicating that the numerical solution was independent of the mesh density. Therefore, the fine mesh was selected for all subsequent simulations. Owing to variations in the jet-to-wall distance, the total number of mesh elements ranged from approximately 500,000 to 600,000 across the remaining cases, while maintaining the same meshing strategy.

Table 1. Mesh independence study performed for the H/D = 6 and θ = 60° configuration

Mesh	Number of elements	Average nusselt number	Relative difference (%)
Coarse	298,416	6.764	-
Medium	426,573	6.812	0.71
Fine	557,842	6.830	0.26

Element quality is one of the primary mesh quality metrics used to evaluate the geometric suitability of the computational mesh for numerical simulations. It is determined by geometric characteristics such as element shape, edge length distribution, internal angles, and node arrangement, all of which influence the accuracy and numerical stability of the solution [20]. In general, the element quality index ranges from 0 to 1, where values closer to 1 indicate elements with a geometry closer to the ideal shape. A high-quality mesh reduces discretization errors, thereby improving solution accuracy and numerical robustness. In the present study, more than 90% of the computational elements exhibited element quality values between 0.9 and 1.0, demonstrating the excellent geometric quality of the generated mesh. The detailed element quality distribution is summarized in Table 2, confirming that the adopted mesh is suitable for accurate and reliable CFD simulations.

Table 2. Element quality distribution of computational mesh

Element quality range	Number of elements	Percentage (%)
0.0 ----- 0.1	13,946	2.5
0.1 ----- 0.2	11,156	2.00
0.2 ----- 0.3	8,367	1.50
0.3 ----- 0.4	6,694	1.20
0.4 ----- 0.5	5,578	1.00
0.5 ----- 0.6	4,462	0.80
0.6 ----- 0.7	2,789	0.50
0.7 ----- 0.8	1,673	0.30
0.8 ----- 0.9	1,115	0.20
0.9 ----- 1.0	502,057	90.00

Skewness is one of the most widely used mesh quality metrics for evaluating the geometric distortion of computational mesh elements. It quantifies the deviation of an element from its ideal shape and directly influences the numerical accuracy, stability, and convergence of CFD simulations [21]. In general, skewness values range from 0 to 1, with lower values indicating higher-quality elements and lower geometric distortion. Conversely, high skewness values may increase discretization errors and reduce numerical accuracy. In the present study, the generated computational mesh exhibited an average skewness value of 0.13, indicating excellent mesh quality. Furthermore, the detailed skewness distribution presented in Table 3 shows that many of the elements possess skewness values below 0.2, confirming that the generated mesh provides excellent numerical quality for the present simulations.

Table 3. Skewness distribution of computational mesh

Skewness range	Number of elements	Percentage (%)
0.0 ----- 0.1	334,705	60.00
0.1 ----- 0.2	172,931	31.00
0.2 ----- 0.3	27,892	5.00
0.3 ----- 0.4	11,156	2.00
0.4 ----- 0.5	5,578	1.00
0.5 ----- 0.6	2,789	0.50
0.6 ----- 0.7	1,673	0.30
0.7 ----- 0.8	836	0.15
0.8 ----- 0.9	278	0.05
0.9 ----- 1.0	0	0.00

To further evaluate the near-wall mesh resolution, the area-weighted average wall y^+ on the heated surface was monitored throughout the numerical solution, as shown in Figure 3. The area-weighted average wall y^+ initially increased during the early iterations, reached a maximum value of approximately 0.32, and then gradually decreased as the solution converged. After 5000 iterations, the monitored wall y^+ stabilized at approximately 0.265, while the minimum value observed during the solution process was approximately

0.04. Since both the peak and converged wall y^+ values remained well below the SST k–ω turbulence model's recommended limit of $y < 1$, the adopted near-wall mesh provides sufficient resolution to accurately capture the viscous sublayer without relying on wall functions, thereby confirming its suitability for the present numerical simulations.

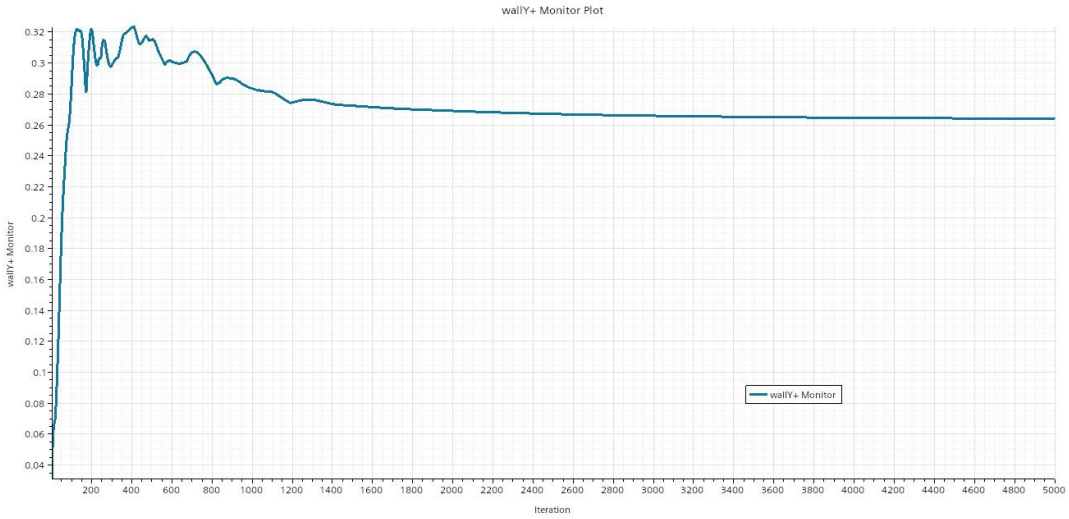


Figure 3. Convergence history of the area-weighted average wall y^+ on the heated surface (H/D = 6, θ = 60°)

2.3. CFD Modeling

In this study, numerical analyses have been performed using CFD software. Solutions have been implemented for steady-state flow conditions under pressure-based formulation. Air has been selected as the fluid medium, assumed to be incompressible and Newtonian. Radiation effects have been neglected, and only conduction and convection mechanisms have been considered. The SST k–ω turbulence model has been used in all analyses. This turbulence model has been selected because it combines the advantages of the standard k–ω model in the near-wall region with those of the k–ε model in the free-stream region. Jet impingement flows are characterized by strong adverse pressure gradients, flow separation, and complex near-wall turbulent structures. Therefore, the SST k–ω model has been widely recommended for accurately predicting wall-bounded flows and heat transfer characteristics. Furthermore, previous numerical studies [22,23] have demonstrated that the SST k–ω model provides better agreement with experimental data than commonly used eddy-viscosity models, including the Standard k–ε, RNG k–ε, and Realizable k–ε models.

The SST k–ω turbulence model solves two additional transport equations: one for the turbulent kinetic energy (k) and one for the specific dissipation rate (ω). The transport equations can be expressed as follows:

$$\frac{\partial(\rho k)}{\partial t}+\frac{\partial(\rho u_i k)}{\partial x_i}=P_k-\beta^*\rho k\omega+\frac{\partial}{\partial x_i}\left[(\mu+\sigma_k\mu_t)\frac{\partial k}{\partial x_i}\right] \quad (1)$$

$$\frac{\partial(\rho\omega)}{\partial t}+\frac{\partial(\rho u_i \omega)}{\partial x_i}=\alpha\frac{\omega}{k}P_k-\beta\rho\omega^2+\frac{\partial}{\partial x_i}\left[(\mu+\sigma_\omega\mu_t)\frac{\partial\omega}{\partial x_i}\right]+2(1-F_1)\frac{\rho\sigma_{\omega^2}}{\omega}\frac{\partial k}{\partial x_i}\frac{\partial\omega}{\partial x_i} \quad (2)$$

where P_k is the turbulence production term, μ_t is the turbulent eddy viscosity, and F_1 is the blending function that combines the standard k–ω formulation near the wall with the k–ε formulation in the free-stream region. Owing to this blending strategy, the SST k–ω model provides improved predictions for adverse pressure gradients, flow separation, and near-wall heat transfer, making it particularly suitable for jet impingement cooling applications.

The wall convergence resolution for the turbulence solution has been provided with $y^+ < 1$. The SIMPLE algorithm has been employed for pressure-velocity coupling, and the Second-Order Upwind scheme has been utilized for discretization. Convergence criteria have been set at 10^{-6} for the energy equation and 10^{-4} for all other equations. Each simulation was continued until all residuals satisfied the prescribed

convergence criteria and the monitored thermal quantities (e.g., average Nusselt number) exhibited negligible variation with further iterations. The designed model specified the following boundary conditions: the jet exit as a velocity inlet, the exit as a pressure outlet, the target surface as a heat flux wall, and the other surfaces as adiabatic walls. Figure 4 illustrates the boundary conditions applied in the numerical model.

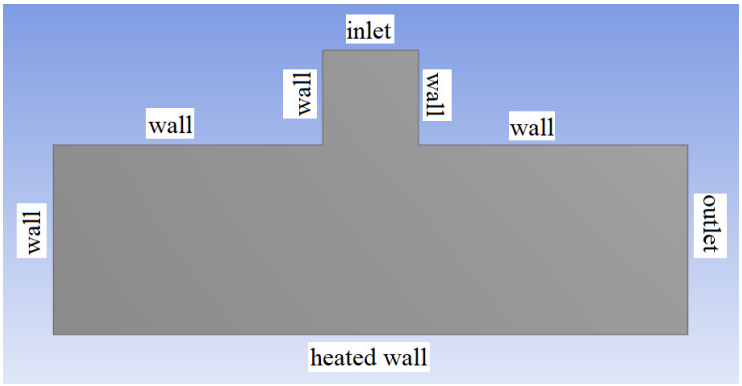


Figure 4. Boundary conditions of the computational domain

The heat flux applied to the target surface has been maintained at 500 W/m² in all analyses. The air inlet temperature has been assumed to be 300 K, and the target wall ambient temperature has been set to 300 K. A constant Reynolds number of 15,000 was selected throughout the study to isolate the effects of jet inclination angle and jet-to-wall distance on heat transfer performance without introducing additional flow-dependent variables. This Reynolds number lies within the turbulent flow regime commonly employed in previous experimental and numerical investigations of jet impingement cooling [24,25] and is representative of practical engineering applications requiring high convective heat transfer rates. The jet-wall distance has been varied at H/D = 3, 4, 5, and 6, and the jet inclination angle has been varied at 0°, 15°, 30°, 45°, and 60°. Thus, a total of 20 different analyses has been performed. The obtained solutions have been evaluated after thermal equilibrium has been reached, and for each case, the Nusselt number (Nu), heat transfer coefficient (h), and wall temperature distribution results have been calculated in the CFD-Post environment.

A two-dimensional steady-state formulation was adopted to enable a systematic comparison of different jet inclination angles and H/D ratios under identical operating conditions while maintaining a reasonable computational cost. Although jet impingement flow is inherently three-dimensional and unsteady, previous studies have shown that two-dimensional steady-state RANS simulations can provide reliable predictions of the overall flow characteristics and average heat transfer performance for single-jet impingement configurations. Therefore, the present approach was considered appropriate for evaluating the relative influence of the investigated geometric parameters rather than resolving transient three-dimensional flow structures.

Since a steady-state pressure-based solver was employed, the Courant–Friedrichs–Lewy (CFL) condition has not been applicable. Numerical stability has been assessed through the convergence of the residuals and the stabilization of the monitored solution variables.

3. RESULTS

3.1. Effects of H/D Ratio and Jet Inclination Angle on Nusselt Number and Heat Transfer Coefficient

The heat transfer coefficient (h) and Nusselt number (Nu) were compared for different jet-to-wall distance ratios (H/D) and jet inclination angles to investigate the influence of geometric parameters on heat transfer performance. Figure 5 illustrates the variation of the Nusselt number with H/D ratio for different jet inclination angles.

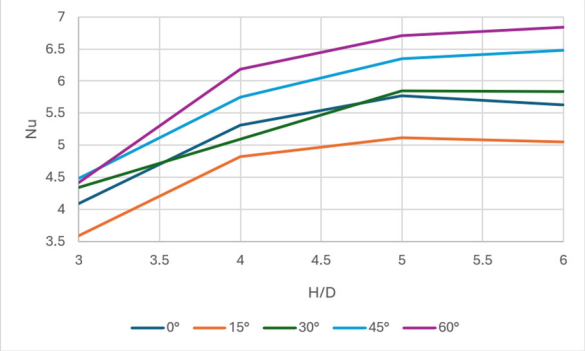


Figure 5. Nusselt number variation depending on H/D ratio for different jet inclination angles

The Nusselt number consistently increases with increasing H/D ratio for all jet inclination angles. At θ = 0°, the Nu value increases from 4.09 to 5.63 as the H/D ratio increases from 3 to 6, while at θ = 60°, it increases from 4.42 to 6.83. This behavior can be attributed to the increased jet development distance before impingement, which is likely to promote stronger turbulence and more effective momentum transfer over the heated surface.

Consequently, heat transfer is enhanced as the wall-jet region becomes more effective. Figure 4 also demonstrates the significant influence of jet inclination angle. Although only a limited improvement is observed at low inclination angles (0°–15°), the Nusselt number increases considerably at 45° and 60°. For example, at H/D = 5, the Nu value increases from 5.77 at θ = 0° to 6.70 at θ = 60°. This enhancement can be attributed to the stronger wall-parallel flow generated by the inclined jet, which is likely to enhance near-wall mixing and improve thermal transport. Overall, the combined increase in H/D ratio and jet inclination angle leads to a substantial improvement in heat transfer performance. The highest Nusselt number (Nu = 6.83) is obtained at H/D = 6 and θ = 60°, corresponding to an approximately 67% increase compared with the vertical jet configuration at H/D = 3. These findings are in good agreement with previous studies, which also reported that larger jet inclination angles and appropriate jet-to-wall distances improve the overall heat transfer performance of jet impingement cooling systems [26,27].

The variation of the Nusselt number with jet inclination angle for different H/D ratios is shown in Figure 6.

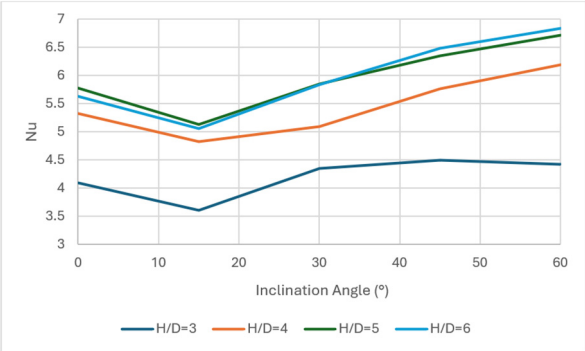


Figure 6. Effect of jet inclination angle on nusselt number for different H/D Ratios

Consistent with the results presented in Figure 4, the Nusselt number increases with increasing jet inclination angle, and this enhancement becomes more pronounced as the H/D ratio increases. At H/D = 3, the influence of jet inclination is relatively limited, with the Nu value increasing from 4.09 at θ = 0° to 4.48 at θ = 45°. In contrast, at H/D = 6, the Nusselt number increases from 5.63 at θ = 0° to 6.83 at θ = 60°, corresponding to an improvement of approximately 21%. These results indicate that the beneficial effect of jet inclination becomes more significant when the jet has sufficient distance to develop before impingement.

Moreover, the Nusselt numbers at H/D = 5 and 6 are very close, suggesting that a jet-to-wall distance of H/D = 5–6 provides the most favorable thermal performance among the investigated cases. At lower H/D

ratios, limited jet development before impingement limits overall heat transfer performance. Therefore, the combination of H/D = 5–6 and θ = 60° provides the most favorable thermal performance among the investigated cases. These observations are consistent with previous studies, which also reported that increasing the jet inclination angle enhances convective heat transfer under appropriate jet-to-wall spacing conditions [28,29].

Figure 7 shows the variation of the heat transfer coefficient (h) with jet inclination angle for different H/D ratios.

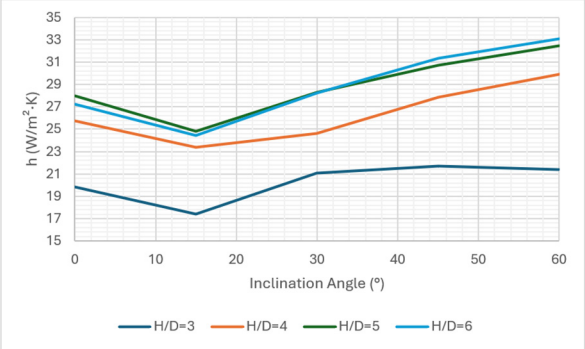


Figure 7. Effect of Jet Inclination Angle on Convective Heat Transfer Coefficient

Like the Nusselt number results, the heat transfer coefficient generally increases with increasing H/D ratio and jet inclination angle. At H/D = 3, the influence of jet inclination is limited, and the heat transfer coefficient decreases slightly from 19.8 W/m²K to 17.4 W/m²K as the inclination angle increases from 0° to 15°, followed by a gradual recovery at higher inclination angles. In contrast, the beneficial effect of jet inclination becomes more evident at larger H/D ratios. For H/D = 5, the heat transfer coefficient increases from 27.9 W/m²K to 32.46 W/m²K, while for H/D = 6 it increases from 27.72 W/m²K to 33.08 W/m²K as the inclination angle increases from 0° to 60°, corresponding to an improvement of approximately 18–20%. These trends are consistent with the Nusselt number results presented in Figs. 4 and 5, confirming that larger jet-to-wall distances enhance the effectiveness of jet inclination on heat transfer performance. Overall, the highest heat transfer coefficients are obtained at H/D = 5–6 and inclination angles of 45°–60°, indicating that these conditions provide the most favorable thermal performance among the investigated cases. The numerical results also agree with similar studies reported in the literature [28-30].

3.2. Temperature Distribution and Flow Structure Ana

Temperature contours obtained for different H/D ratios and jet inclination angles were analyzed to investigate the influence of flow structure on the surface temperature distribution. Figure 8 shows the temperature contours for H/D = 3 at jet inclination angles of θ = 0°, 15°, 30°, 45°, and 60°.

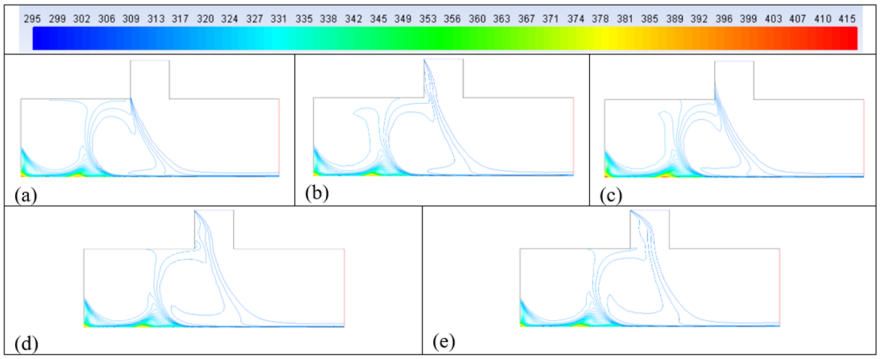


Figure 8. Temperature contours for H/D = 3 at different jet inclination angles: (a) θ = 0°, (b) θ = 15°, (c) θ = 30°, (d) θ = 45°, (e) θ = 60°

At this relatively small jet-to-wall distance, the jet impinges on the heated surface before it is fully developed, resulting in a highly localized thermal field. For the vertical jet (θ = 0°), the low-temperature

region is concentrated around the stagnation point, producing steep temperature gradients near the wall and limiting the cooling effect to a relatively small area. As the jet inclination angle increases to 15° and 30°, the cooled region gradually extends downstream, leading to a more uniform temperature distribution over the heated surface. Further increases in the inclination angle to 45° and 60° enlarge the thermal interaction region, resulting in a more homogeneous temperature field and lower wall temperatures. This behavior indicates that inclined jets improve the overall cooling performance by distributing the cooling effect over a larger surface area rather than concentrating it near the stagnation point. Consequently, the temperature contours support the Nusselt number results presented in the previous section, which showed that higher jet inclination angles provide superior overall heat transfer performance.

Figure 9 shows the temperature contours for H/D = 4 at jet inclination angles of θ = 0°, 15°, 30°, 45°, and 60°.

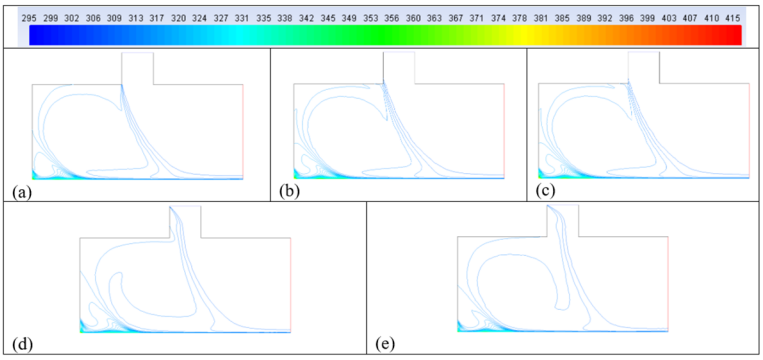


Figure 9. Temperature contours for H/D = 4 at different jet inclination angles: (a) θ = 0°, (b) θ = 15°, (c) θ = 30°, (d) θ = 45°, (e) θ = 60°

Compared with the H/D = 3 configuration, the increased jet-to-wall distance provides additional space for jet development before impingement, resulting in a more uniform temperature distribution over the heated surface. At θ = 0°, the cooling effect remains concentrated around the stagnation region, although the temperature gradients become less localized than those observed at H/D = 3. As the inclination angle increases, the cooled region progressively extends along the wall, producing a more homogeneous thermal field. The effect becomes more pronounced at θ = 45° and 60°, where the temperature contours cover a larger portion of the heated surface, indicating improved cooling uniformity. Overall, the H/D = 4 configuration provides a more balanced temperature distribution than H/D = 3, while the beneficial influence of jet inclination becomes increasingly evident. These observations are consistent with the improvements in Nusselt number reported in the previous section.

Figure 10 shows the temperature contours for H/D = 5 at jet inclination angles of θ = 0°, 15°, 30°, 45°, and 60°.

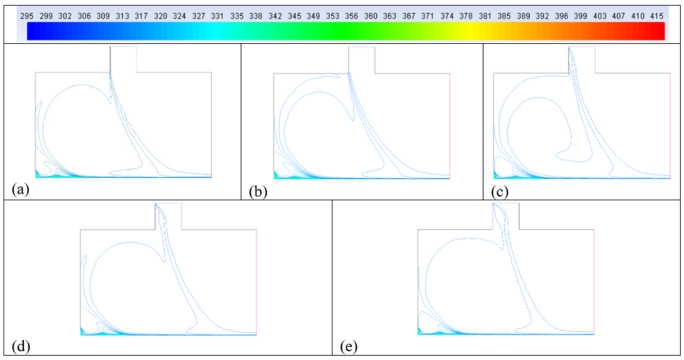


Figure 10. Temperature contours for H/D = 5 at different jet inclination angles: (a) θ = 0°, (b) θ = 15°, (c) θ = 30°, (d) θ = 45°, (e) θ = 60°

Compared with the H/D = 3 and H/D = 4 configurations, the temperature distribution becomes noticeably more uniform, indicating that the increased jet-to-wall distance allows the jet to impinge on the heated

surface under more favorable conditions. At θ = 0°, the cooling effect remains concentrated near the stagnation region, whereas increasing the inclination angle progressively enlarges the cooled area along the heated surface. The improvement becomes particularly evident at θ = 45° and 60°, where the temperature contours indicate lower wall temperatures and a more homogeneous thermal field. These observations are consistent with the increase in Nusselt number and heat transfer coefficient presented in the previous section. Overall, the H/D = 5 configuration represents one of the most favorable operating conditions, providing an effective balance between jet development and heat transfer performance.

Figure 11 shows the temperature contours for H/D = 6 at jet inclination angles of θ = 0°, 15°, 30°, 45°, and 60°.

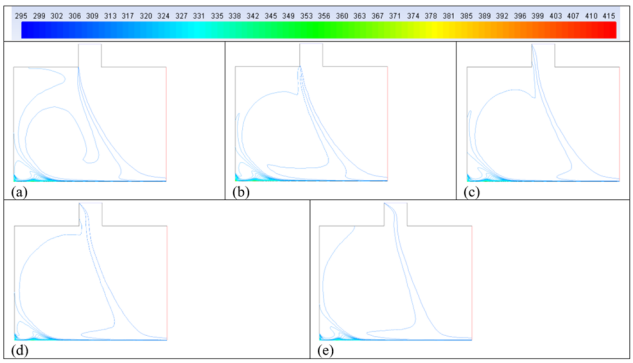


Figure 11. Temperature contours for H/D = 6 at different jet inclination angles: (a) θ = 0°, (b) θ = 15°, (c) θ = 30°, (d) θ = 45°, (e) θ = 60°

Among the investigated configurations, H/D = 6 exhibits the most uniform temperature distribution, indicating that a larger jet-to-wall distance provides additional jet development before impingement. At θ = 0°, the cooling effect remains concentrated near the stagnation region, whereas increasing the jet inclination angle progressively enlarges the cooled area along the heated surface. The temperature contours become increasingly uniform at θ = 45° and 60°, demonstrating that the inclined jet provides more effective cooling over a wider surface area. Consequently, the lowest wall temperatures are observed under these conditions, consistent with the highest Nusselt numbers and heat transfer coefficients reported in the previous section. Overall, the H/D = 6 configuration provides the most favorable thermal performance among the investigated cases, indicating that a sufficiently developed jet combined with a large inclination angle is associated with improved cooling effectiveness in the impingement system.

These findings are also consistent with recent numerical and experimental studies demonstrating that geometric configuration and airflow conditions play a decisive role in convective cooling performance and temperature uniformity [31,32].

4. CONCLUSIONS

In this study, the heat transport performance of jet impingement cooling systems has been investigated using CFD for different jet inclination angles (0°, 15°, 30°, 45°, and 60°) and jet-to-wall distances (H/D = 3, 4, 5, and 6). The numerical results indicate that both the H/D ratio and the jet inclination angle significantly influence heat transfer performance. As the H/D ratio increases, both the heat transfer coefficient (h) and the Nusselt number (Nu) increase. For H/D = 3, the average Nusselt number ranges from approximately 4.09 to 4.49, while the heat transfer coefficient varies between 19.82 and 21.05 W/m²K. In contrast, for H/D = 6, these values increase to approximately 5.05–6.83 and 24.44–33.08 W/m²K, respectively. This trend can be attributed to the longer jet development distance and the resulting improvement in flow development before impingement.

Similarly, increasing the jet inclination angle improves the predicted cooling performance. At a vertical jet configuration (0°), the lowest average Nusselt number is approximately 4.09, whereas the highest value (approximately 6.83) is obtained at an inclination angle of 60°, corresponding to an improvement of approximately 67%. The numerical results suggest that increasing the jet inclination angle is associated with stronger secondary vortical structures, thereby enhancing turbulent mixing near the heated surface and

improving convective heat transfer. According to the numerical results, the highest cooling performance is obtained at H/D = 5–6 and jet inclination angles of 45°–60°. The present study systematically evaluates the combined influence of the jet inclination angle and the H/D ratio while maintaining a constant Reynolds number, providing useful guidance for the design and optimization of inclined-jet impingement cooling systems.

Nevertheless, the present study has some limitations. The numerical analyses were performed using a two-dimensional steady-state CFD model to enable a systematic parametric investigation with reasonable computational cost. Although this approach cannot fully account for the inherently three-dimensional and unsteady characteristics of jet impingement flow, including complex vortex structures and transient turbulent fluctuations, it is considered appropriate for comparative evaluation of the investigated geometric parameters and provides meaningful insight into the thermal behavior of inclined jet impingement systems. In addition, no experimental validation was performed for the specific configuration investigated in the present study, which is a limitation of this work. Therefore, the numerical results should be interpreted within the scope of the adopted numerical model. Future studies will focus on experimental validation of the proposed configuration and on extending the model to three-dimensional transient simulations.

5. REFERENCES

1. Ekkad, S.V. & Singh, P. (2021). A modern review on jet impingement heat transfer methods. *Journal of Heat Transfer, 143*(6), 064001.
2. Wen, Y., Li, Y., Li, J. & Yu, X. (2023). Numerical investigation of jet impingement cooling with supercritical pressure carbon dioxide in a multi-layer cold plate during high heat flux. *Journal of Thermal Science, 32*, 237-253.
3. Dutta, S. & Singh, P. (2021). Opportunities in jet-impingement cooling for gas-turbine engines. *Energies, 14*(20), 6587.
4. Bu, X., Peng, L., Lin, G., Bai, L. & Wen, D. (2015). Experimental study of jet impingement heat transfer on a variable-curvature concave surface in a wing leading edge. *International Journal of Heat and Mass Transfer, 90*, 92-101.
5. Xu, L., Hu, N., Lin, H., Xi, L., Li, Y. & Gao, J. (2024). A review of flow field and heat transfer characteristics of jet impingement from special-shaped holes. *Energies, 17*(1), 4510.
6. Alnak, D.E. ve Karabulut, K. (2021). Jet giriş genişliğinin ısı transferi ve akış yapısına olan etkisinin araştırılması. *Çukurova Üniversitesi Mühendislik Fakültesi Dergisi, 36*(2), 331-345.
7. Yang, X., Wu, H. & Feng, Z. (2022). Jet impingement heat transfer characteristics with variable extended jet holes under strong crossflow conditions. *Aerospace, 9*(1), 44.
8. Cademartori, S., Cravero, C., Marini, M. & Marsano, D. (2021). CFD simulation of the slot jet impingement heat transfer process and application to a temperature control system for galvanizing line of metal band. *Applied Sciences, 11*, 1149.
9. Lin, Z.H., Chou, Y.J. & Hung, Y.H. (1997). Heat transfer behaviors of a confined slot jet impingement. *International Journal of Heat and Mass Transfer, 40*(5), 1095-1107.
10. Kaewchoothong, N., Nuntadusit, C. & Chatpun, S. (2025). Effect of jet-to-target spacing on flow and heat transfer characteristics for swirling impinging micro-slot jets. *Heat Transfer Engineering, 46*(1), 1371-1384.
11. Keleş, H. ve Özmen, Y. (2024). 45° eğimli ikincil jetlere sahip sınırlandırılmamış ve sınırlandırılmış çarpan jet dizilerinde ısı transferi karakteristiklerinin deneysel incelenmesi. *Çukurova Üniversitesi Mühendislik Fakültesi Dergisi, 39*(4), 923-937.
12. Benmouhoub, D. & Mataoui, A. (2013). Turbulent heat transfer from a slot jet impinging on a flat plate. *Journal of Heat Transfer, 135*(1), 102201.
13. Singh, P., Grover, N.K., Agarwal, V., Sharma, S., Singh, J., Sadeghzadeh, M. & Issakhov, A. (2021). Computational fluid dynamics analysis of impingement heat transfer in an inline array of multiple jets. *Mathematical Problems in Engineering, 2021*(1), 6668942.
14. Shin, M.-S., Senguttuvan, S. & Kim, S.-M. (2021). Investigations of flow and heat transfer characteristics in a channel impingement cooling configuration with a single row of water jets. *Energies, 14*(1), 4327.
15. Olsson, E.E.M., Ahrné, L.M. & Tragardh, A.C. (2004). Heat transfer from a slot air jet impinging on a circular cylinder. *Journal of Food Engineering, 63*(1), 393-401.
16. Culun, P., Celik, N. & Pihtili, K. (2018). Effects of design parameters on a multi jet impinging heat transfer. *Alexandria Engineering Journal, 57*(1), 4255-4266.

17. Kumar, A., Maithani, R., Sharma, S., Srivastav, A., Alam, T., Siddiqui, M.I.H., Dobrotă, D., Cofaru, N.-F. & Ashraf, I. (2025). Impact of straight slot impingement jets on heat transfer enhancement of TiO_2/H_2O nanofluid flow in a square channel: CFD analysis. *Scientific Reports, 15*(1), 7728.
18. Molana, M. & Banooni, S. (2013). Investigation of heat transfer processes involved liquid impingement jets: A review. *Brazilian Journal of Chemical Engineering, 30*(3), 413-435.
19. Uddin, N., Kee, P.T.W. & Weigand, B. (2024). Heat transfer by jet impingement: A review of heat transfer correlations and high-fidelity simulations. *Applied Thermal Engineering, 257*(1), 124258.
20. Xie, J., Yang, X., Du, Y., Zhou, P., Cao, J., Zhou, Y. & Guan, Z. (2026). Voronoi-based high-quality mesh refinement for tetrahedral mesh generation. *Computers and Structures, 321*, 108114.
21. Kim, I., Chae, J. & You, D. (2025). Automatic mesh generation for optimal CFD of a blade passage using deep reinforcement learning. *Journal of Computational Physics, 541*, 114306.
22. Thakar, S.S., Nambiar, S., Chandavarkar, G.A. & Prabu, S.S. (2021). Investigation of impingement cooling on a heat sink using CFD simulation. *Materials Today: Proceedings, 46*(1), 8753-8760.
23. Steyn, G., Vermeulen, C. & Steyn, M. (2020). Multi-jet gas cooling of in-beam foils or specimens: CFD predictions of the convective heat-transfer coefficient. *EPJ Web of Conferences, 229*(1), 05002.
24. Peteinaris, A., Celik, A., Cukurel, B. & Terzis, A. (2026). Experimental validation of Reynolds–Prandtl scaling for confined gas jet impingement heat transfer. *Journal of Thermal Science and Engineering Applications, 18*(7), 071007.
25. Wang, C., Luo, L., Wang, L. & Sundén, B. (2016). Effects of vortex generators on the jet impingement heat transfer at different cross-flow Reynolds numbers. *International Journal of Heat and Mass Transfer, 96*(1), 278-286.
26. Lak, A., Çalışır, T. & Başkaya, Ş. (2020). Flow and heat transfer characteristics of inclined jet impingement on a flat plate. *Politechnic Journal, 23*(1), 697-706.
27. Wang, X.L., Yan, H.B., Lu, T.J., Song, S.J. & Kim, T. (2014). Heat transfer characteristics of an inclined impinging jet on a curved surface in crossflow. *Journal of Heat Transfer, 136*(1), 081702.
28. Ramezanpour, A., Shirvani, H. & Mirzaee, I. (2004). Heat transfer modelling of slot jet impinging on an inclined plate. *Heat Transfer VIII,* 485-494.
29. Karabey, A. & Yorulmaz, D. (2025). Experimental analysis of heat and flow characteristics on inclined and multiple impingement jet heat transfer using optimized heat sink. *Applied Sciences, 15*(1), 2657.
30. Akansu, Y.E., Sarioglu, M., Kuvvet, K. & Yavuz, T. (2008). Flow field and heat transfer characteristics in an oblique slot jet impinging on a flat plate. *International Communications in Heat and Mass Transfer, 35*(1), 873-880.
31. Karabulut, K. ve Alnak, Y. (2023). Kanaldaki jet akış sayısına bağlı olarak farklı model yüzeylerinden olan ısı transferi ve akış yapısının analizi. *Çukurova Üniversitesi Mühendislik Fakültesi Dergisi, 38*(1), 49-60.
32. Akkuş, F. ve Işık, M.Z. (2025). Boru destekli hava soğutmalı sistemlerin lityum-iyon batarya paketlerindeki termal performansının incelenmesi. *Çukurova Üniversitesi Mühendislik Fakültesi Dergisi, 40*(4), 855-866.